JOURNAL OF GEOPHYSICAL RESEARCH, VOL. 101, NO. B8, PAGES 17,523–17,533, AUGUST 10, 1996

Pressure dependence of velocity and attenuation and its relationship to crack closure in crystalline rocks

I. L. Meglis[1], R. J. Greenfield, T. Engelder, and E. K. Graham

Department of Geosciences, The Pennsylvania State University, University Park

Abstract. Measurements of linear strain, ultrasonic velocity, and attenuation (Q^{-1}) were made simultaneously as functions of confining pressure on core and outcrop samples from the Moodus, Connecticut, area. Strain measurements indicate the core samples contain cracks which formed in part by stress relief during recovery (Meglis et al., 1991). The outcrop samples have a small crack porosity compared with the cores. Closure of cracks with increasing confining pressure causes an increase in velocity and a decrease in attenuation. We present a form for the pressure dependence of the crack density parameter ε (the number of cracks of unit radius per unit volume), which was used to incorporate the influence of crack closure with pressure into models of wave velocity and attenuation in cracked solids. The crack density parameter is represented as an exponentially decreasing function of confining pressure. The pressure dependence of ε was determined from the strain measurements using the non-self-consistent effective modulus approach of O'Connell and Budiansky (1974), from the velocity data using the solutions of Garbin and Knopoff (1973) and Hudson (1981), and from the attenuation measurements using the frictional attenuation model of Walsh (1966). All of the models fit the data reasonably well using an exponentially decaying ε described by one decay constant τ. However, some of the data are better fit by a crack density parameter with two decay constants, reflecting a rapid decrease of ε at low pressure and a slower decrease at higher pressure. There is considerable variation among the predicted decay constants for a given sample from the different data sets. Several factors contribute to this variation. For example, the two velocity models predict a different dependence of velocity on ε, which results in a different dependence of ε on pressure. For the Q^{-1} data, approximating $d\varepsilon/dP$ by a function with a single decay constant results in lower τ values for Q^{-1} than for strain or velocity. Finally, a large anisotropy in attenuation measured in the deepest core samples indicates that scattering is a significant source of wave energy loss in these samples, and therefore a frictional attenuation mechanism alone cannot account for all the observed attenuation.

Introduction

The velocities and amplitudes of elastic waves propagating through rocks are strongly affected by the presence of cracks. An understanding of the interaction between elastic waves and cracks follows in part from theoretical models which account for the changes in velocity and attenuation (Q^{-1}) caused by the addition of cracks to initially intact samples [*Walsh*, 1966; *Garbin and Knopoff*, 1973; *O'Connell and Budiansky*, 1974; *Garbin and Knopoff*, 1975a,b; *Crampin et al.*, 1980; *Hudson*, 1981; *Kikuchi*, 1981; *Crampin*, 1984; *Sayers*, 1988]. The characteristics of the crack population are incorporated into velocity and attenuation models using the crack density parameter ε, which is defined as $\varepsilon = n \langle r^3 \rangle$ [*Walsh*, 1966], where n is the number of open cracks of radius r per unit volume of rock. The value of the crack density parameter for a given rock sample can be calculated directly from linear strain-pressure data [*Wang and Simmons*, 1978].

The pressure dependence of velocity and attenuation in dry samples subjected to confining pressure arises primarily from the closure of cracks. As pressure is applied the number (n) of open cracks decreases, causing a corresponding increase in wave velocities and, depending on the attenuation mechanism, either an increase or a decrease in wave amplitudes. Crack closure is represented numerically by a decreasing ε. In this paper we present a form for the pressure dependence of ε, based on analysis of linear strain-pressure data for a suite of crystalline rock samples subjected to confining pressures up to 140-150 MPa. We use this function $\varepsilon(P)$ to incorporate the effects of crack closure into models for velocity and attenuation and then use these models to fit velocity and attenuation data collected simultaneously with linear strain in our samples. Our primary objective is to compare the pressure dependence of $\varepsilon(P)$, computed from models fit to the three data sets from each sample. We note that *Carlson and Gangi* [1985] present a theoretical derivation and *Wepfer and Christensen* [1991] present an empirical relation, both of which describe the pressure dependence of velocity but do not explicitly incorporate the crack density parameter.

The amplitudes and velocities of elastic waves in rocks are affected by such factors as the size, density, orientation distribution, geometry, and surface roughness of cracks [*Walsh*, 1966; *Friedman and Bur*, 1974; *Lockner et al.*, 1977;

[1]Now at Faculty of Engineering and Applied Science, Memorial University of Newfoundland, St. John's, Canada.

Paper number 96JB00107.
0148-0227/96/96JB-00107$09.00

Winkler and Nur, 1979; *Cheng and Toksoz*, 1979; *Johnston and Toksoz*, 1980; *Murphy*, 1984; *Pyrak-Nolte et al.*, 1990; *Coyner and Martin*, 1990; *Sayers et al.*, 1990]. These characteristics are, in part, related to the stress history of the samples [*Douglass and Voight*, 1969; *Hadley*, 1976; *Engelder*, 1984; *Engelder and Plumb*, 1984; *Carlson and Wang*, 1986; *Meglis et al.*, 1991]. Core samples used in this study were initially subjected to mean stress magnitudes ranging from 5 to 60 MPa. Core recovery induced both rapid stress relief and a transient high horizontal stress concentration, causing relatively high crack porosities in these samples. Outcrop samples, in contrast, were subjected to lower mean stress levels and were not affected by the stress concentration associated with drilling. While the outcrop samples, like the core samples, experienced large amounts of stress relief, that relief occurred gradually during geologic unloading over a long time period. As a consequence, the outcrop samples contain much lower crack porosities than do the cores. Given their different stress histories, we expect the core samples to have a significant population of fresh, sharp-tipped, stress-induced cracks with well-matched faces, whereas the outcrop samples are more likely to have older, healed or partially healed cracks. Previous work indicates that fresh, stress-induced cracks have a low aspect ratio (the ratio of crack aperture to length) and therefore close at low confining pressure, whereas higher aspect ratio pores and healed cracks can persist to high pressures [*Batzle et al.*, 1980; *Hadley*, 1976; *Carlson and Wang*, 1986]. Therefore variations in the pressure dependence of ε should reflect the behavior of cracks with different aspect ratios in response to the confining pressure. We discuss the results of our analysis in the context of the different stress histories of the core and outcrop samples.

Procedure

Sample Description

Cores were recovered from the Moodus (Connecticut) borehole at intervals of approximately 150 m to a maximum depth of 1356 m [*Woodward-Clyde Consultants*, 1988] (Table 1). The upper half of the 1356-m borehole is within the Merrimack terrane; core samples of the Hebron formation from this terrane are predominantly medium-grained quartz-plagioclase-biotite gneisses. The lower half of the borehole intersects Precambrian age metavolcanics of the Avalon terrane; core samples from the Waterford formation of this terrane are predominantly medium-grained quartz-plagioclase-amphibole-biotite gneisses and fine-grained amphibolite. All the samples have a subhorizontal metamorphic foliation which has influenced the orientation of recovery-induced microcracks [*Meglis et al.*, 1991]. Three outcrop samples collected from the Moodus area, two from the Waterford formation and one from the Hebron formation, were analyzed for comparison with cores from the equivalent formation recovered at depth in the Moodus borehole. The outcrop samples chosen showed minimal superficial weathering, and test specimens were cut from the centers of larger blocks so that in general several centimeters of exposed material were removed.

Sample Preparation

Samples were cut into blocks of approximately 50 mm sides with one axis [z] parallel to the vertical direction in the core specimens. The two vertical faces were cut parallel to N80°E, the approximate trend of *SH* (the maximum horizontal stress) determined in the Moodus well, and to N170°E, the trend of *Sh* (the minimum horizontal stress) [*Plumb and Hornby*, 1988; *Baumgartner and Zoback*, 1989]. These directions are designated [x] (*SH*) and [y] (*Sh*). Samples were ground using a surface grinder and then dried under a vacuum at ambient temperature for 24 hours.

Three 45° linear strain gage rosettes were attached, along with four pairs of 1-MHz transducers for time-of-flight measurements (three pairs of PZT compressional and one pair of Lithium Niobate shear transducers). The prepared samples were coated with Dow Corning RTV 3140 Silicone Rubber Sealant to exclude the confining medium (hydraulic oil).

Measurements

Strain and velocity measurements were made at pressure increments of between 5 and 20 MPa, as samples were pressurized from ambient to approximately 140-150 MPa

Table 1. In Situ Depth of Samples Studied, Velocities Measured in Three Directions at Approximately 0, 50, and 140 MPa Applied Confining Pressure, and Sample Crack Porosity at Ambient Confining Pressure

	Core Depth, m	[x]			[y]			[z]			Crack Porosity, %
		0 MPa	50 MPa	140 MPa	0 MPa	50 MPa	140 MPa	0 MPa	50 MPa	140 MPa	
M0:5	surface	4.87	5.81	6.20	4.48	5.57	5.95	3.82	5.16	5.58	0.15
M0:9	surface	5.23	5.86	6.17	5.23	5.93	6.20	3.59	5.15	5.51	0.13
M0:13	surface	6.13	6.86	7.11	6.66	7.14	7.37	5.45	6.60	6.88	0.03
M1	155.6	4.84	5.84	6.20	-	-	-	3.16	5.26	5.61	0.18
M2	305.4	4.31	5.86*	6.38	-	-	-	2.79	5.30*	6.31	0.19
M3#2	460.1	4.67	6.18	6.48	4.37	6.05	6.30	2.27	5.30	5.55	0.29
M4#2	598.1	3.87	5.72	6.14	3.72	5.74	6.14	2.82	5.47	6.05	0.33
M6#2	891.0	3.83	6.01	6.44	3.89	5.90	6.37	2.13	5.71	6.04	0.40
M7	1067.6	4.72	5.84	6.30	-	-	-	3.94	5.55	5.85	0.11
M8	-	-	-	-	-	-	-	0.61	-	-	-
M9A	1354.2	3.76	5.02	6.21	-	-	-	2.03	5.23	5.95	0.53
M9B	1355.6	4.37	5.79	6.63	5.20	6.20	6.83	2.71	5.42	6.11	-

*Measured at 40.7 MPa.

confining pressure. Strain measurements in the [x], [y], and [z] directions were analyzed individually, and then the volumetric strain was determined from the sum of these three measurements. For the velocity measurements, one source transducer was excited with a 0.5-μs pulse at a rate of 200 Hz, and the wave was detected by the receiving transducer on the opposing face. One thousand consecutive traces from the transducer pair were averaged by a Lecroy 9400 125-MHz digital oscilloscope, and the averaged waveforms were stored on a Hewlett Packard PC-305 computer before the next source transducer was excited. Segments of the stored waveforms from 5 to 50 μs posttrigger were Fourier transformed with three-point smoothing to obtain the amplitude spectrum. Four velocity measurements were made, though waveforms for only two P wave propagation directions ([z] and [x]) were analyzed for attenuation. The "average" sample velocity as a function of pressure was determined by averaging the velocities measured in the [x], [y], and [z] directions.

Theoretical Derivations

Strain

At low confining pressure the strain measured in rocks, here termed $e_{ij}(P)$, often increases rapidly with pressure P due to the closure of cracks. Following the development of *Siegfried and Simmons* [1978], the compressibility of the cracked material $\beta_{ij}(P)$ is defined as the pressure derivative of the strain de_{ij}/dP, where in our case compressive strains are positive. The volume compressibility $\beta(P)$ is, in turn, given by de_{ii}/dP (summation implied).

As $\beta_{ij}(P)$ approaches a constant value at higher confining pressures, it reflects the "intrinsic" compressibility of the matrix, $\beta^m{}_{ij}$ (i.e., the compressibility of the rock with cracks closed). The deviation of $e_{ij}(P)$ at low pressure from the trend at high pressure is a measure of the strain contributed by the compression and closure of cracks; the strain due to cracks which remain open at a given pressure is termed the crack strain $\eta_{ij}(P)$. The sum of the crack strains measured in three mutually perpendicular directions [x], [y], and [z] is the volumetric crack strain $\eta(P)$ or the crack porosity for the sample. The compressibility $\beta_{ij}(P)$ is related to the crack strain by

$$\beta_{ij}(P) = \frac{de_{ij}}{dP} = \beta^m{}_{ij} - \frac{d\eta_{ij}}{dP} \tag{1}$$

Using the non-self-consistent energy approach of *O'Connell and Budiansky* [1974], the volume compressibility of the cracked solid can also be written

$$\beta(P) = \beta^m[1 + B\varepsilon(P)] \tag{2}$$

where $\varepsilon(P)$ is the crack density parameter at pressure P and the constant B is a function of the Poisson's ratio of the uncracked solid. The form of (2) also describes the relationship between the linear compressibilities of the rock and matrix, $\beta_{ij}(P)$ and $\beta^m{}_{ij}$, provided that the specimen is approximately isotropic.

For the Moodus samples, $\beta^m{}_{ij}$ was computed for each of three mutually perpendicular strain curves ([x], [y], and [z]), and β^m was computed for the volumetric strain curve using least squares fits to the data between approximately 100 and 140-150 MPa. The crack strains $\eta_{ij}(P)$ were determined from (1). Because $\eta_{ij}(P)$ and $\eta(P)$ are approximately exponentially decreasing functions of confining pressure, we have written them in the form shown here for the volumetric crack strain:

$$\eta(P) = \eta_0 \exp(-P/\tau) \tag{3}$$

where η_0 is the value of $\eta(P)$ at ambient pressure and τ is a decay constant with units of pressure which characterizes the rate at which $\eta(P)$ decreases.

By setting (1) and (2) equal in either the linear or volume form, solving for ε, and substituting the derivative of the crack strain with respect to pressure (computed from (3)), we obtain the relation shown here for the volume form

$$\varepsilon(P) = \left(\frac{\eta_0}{\tau\beta B}\right)\exp(-P/\tau) = \varepsilon_0 \exp(-P/\tau). \tag{4}$$

This relation indicates that the crack density parameter has the same pressure dependence as the crack strain $\eta(P)$, namely, an exponentially decreasing function with decay constant τ. The values of τ and η_0 were determined from (3) using a nonlinear least squares fit to the $\eta_{ij}(P)$ and the $\eta(P)$ data.

In some of the samples it was necessary to fit the data with a function described by two decay constants, which takes the form

$$\varepsilon(P) = \varepsilon_{0_1} \exp(-P/\tau_1) + \varepsilon_{0_2} \exp(-P/\tau_2) \tag{5}$$

This form was used primarily to fit data from the deeper, more highly cracked cores, and reflects a rapid decrease in ε at low pressure and a slower decay at high pressure.

Velocity

We use two approaches to relate the P wave velocity to the crack density parameter, both of which involve expressions correct to first order in ε which relate the velocity to the effective elastic moduli of a solid containing dry, penny-shaped cracks [*Garbin and Knopoff*, 1973, 1975a,b; *Hudson*, 1981]. Neither model assumes any particular pressure dependence for the crack density parameter. We have substituted our (4) and, in certain cases (5), for ε in these models. We show the derivations using (4).

First, *Garbin and Knopoff*'s [1973] relation takes the form

$$V_p(P) = V^m{}_p[1 + C_1\varepsilon_0 \exp(-P/\tau)]^{-1/2} \tag{6}$$

where V_p is the P wave velocity of the material at confining pressure P, $V^m{}_p$ is the "intrinsic" P wave velocity of the intact rock matrix, and C_1 is a function of the elastic properties of the uncracked material. We note that this form is similar to the non-self-consistent relation derived by *O'Connell and Budiansky* [1974]. For the second approach we have substituted (4) for ε in *Hudson's* [1981] derivation and arrive at an equation of the form

$$V_p(P) = V^m{}_p[1 - C_2\varepsilon_0 \exp(-P/\tau)]^{1/2}. \tag{7}$$

Crampin [1984] notes that the equations derived by *Hudson* [1981] and *Garbin and Knopoff* [1973] are equivalent for small values of ε. Equations (6) and (7) were fit to the velocities measured in the [x], [y], and [z] directions and to the average sample velocities using a routine which iteratively adjusts the parameters $V^m{}_p$, $(C_1\varepsilon_0)$ or $(C_2\varepsilon_0)$, and τ to minimize the least squares deviation of the function from the data.

Attenuation

Attenuation calculations. To calculate attenuation (Q^{-1}) from the Moodus data, the following procedure from *Toksoz et al.* [1979] was employed using the amplitude of a silica standard as a reference. The ratio of wave amplitudes in the rock and silica samples is given by

$$\frac{A_{rock}}{A_{silica}} = \left(\frac{\kappa_{rock}}{\kappa_{silica}}\right)\exp(\zeta_{silica}Q_s^{-1} - \zeta_{rock}Q^{-1}) \qquad (8)$$

where A is the amplitude, κ is an unknown constant which includes the unattenuated (initial) wave amplitude, and the loss due to transducer coupling, electronics, and other factors, Q^{-1} is the attenuation of the rock, Q^{-1}_s is the attenuation of the silica and is assumed equal to zero, and $\zeta = (\pi f d/V_p)$, where d is the sample length, f is the frequency, and V_p is the measured compressional wave velocity in either the silica or the rock. Although sample lengths were not identical in these specimens, we are primarily interested in the pressure dependence of Q^{-1}. Edge effects or wave spreading may introduce some error into the absolute value of Q^{-1}. However, this error should not vary strongly with the confining pressure.

If the initial wave amplitudes in the silica and the rock are equal, and variations caused by electronics and transducer coupling affect the measurements equally, then the term $(\kappa_{rock}/\kappa_{silica})$ is approximately equal to one. Therefore the attenuation in the rock Q^{-1} at any pressure P is given by the relation

$$Q^{-1}(P) = -\zeta^{-1}_{rock}(P)\ln\left(\frac{A_{rock}(P)}{A_{silica}(P)}\right). \qquad (9)$$

An alternate method of calculating Q^{-1} was employed for comparison with the values determined by (9). If the attenuation is frequency-independent and Q^{-1}_s of the silica standard is approximately equal to zero, then Q^{-1} can be determined from the slope of the natural log of the spectral ratios over a given frequency range,

$$Q^{-1} = \frac{V_p}{\pi d}\frac{\partial}{\partial f}\left(\frac{A_{silica}(f)}{A_{rock}(f)}\right) \qquad (10)$$

where d is the sample length and V_p is the P wave velocity in the cracked solid [*Toksoz et al.*, 1979]. We have used the slope over a frequency range from 0.6 to 1.6 MHz to calculate Q^{-1} at four confining pressures for two core samples (Table 2). Values calculated from the slope of the spectral ratios (equation (10)) for sample M6#2 and M3#2 are comparable to those calculated from the 1-MHz peak amplitude (equation (9)).

Pressure dependence of frictional sliding attenuation. The attenuation in a rock (Q^{-1}) can be represented as the sum of the attenuation caused by cracks (Q^{-1}_c) (which includes both frictional and scattering attenuation) and the intrinsic attenuation (Q^{-1}_i) caused by other mechanisms such as scattering at grain boundaries:

$$Q^{-1} = Q_c^{-1} + Q_i^{-1}. \qquad (11)$$

For a purely frictional sliding attenuation mechanism, $Q^{-1}_c = Q^{-1}_{cf}$; this term depends on the number and average length of the cracks which close over a given small pressure interval [*Walsh*, 1966]. The crack density parameter ε is a measure of both the number and size of open cracks in the specimen. The derivative of the crack density parameter is then related to the number of cracks and the average size of the cracks which close (i.e., which come into incipient contact) per unit pressure increase. We assume that confining pressure causes closure of cracks parallel to the short axis (i.e., the crack aperture diminishes with no change in crack length). For a rock containing a spectrum of aspect ratios, attenuation by friction should therefore be proportional to the derivative of the crack density parameter evaluated at pressure P. We use an equation similar to equation (2) of *Johnston et al.* [1979] which came from *Walsh* [1966]:

$$Q_{cf}^{-1}(P) = \frac{E}{E^m}\frac{d\varepsilon(P)}{dP}\frac{(1-\bar{\nu})}{(1-2\bar{\nu}^2)}F \qquad (12)$$

where $\bar{\nu}$ is the Poisson's ratio of the cracked solid, E is the Young's modulus of the rock at pressure P, E^m is the "intrinsic" Young's modulus of the intact (uncracked) rock matrix, and F is an unspecified function which represents the dependence of Q^{-1}_{cf} on the coefficient of sliding friction along the crack face, the Poisson's ratio of the uncracked solid, and the orientation of the cracks. By inspection of (12),

Table 2. Comparison of Q^{-1} Values Calculated From the Slope of the Spectral Ratios With Those Calculated From the 1-MHz Peak Amplitude for Two Specimens

	Confining Pressure, MPa			
M3#2 [z] Direction	20	40	100	140
Slope method	0.043	0.039	0.032	0.028
1-MHz peak method	0.031	0.023	0.022	0.021
	Confining Pressure, MPa			
M6#2 [x] Direction	25	35	100	140
Slope method	0.083	0.068	0.040	0.028
1-MHz peak method	0.090	0.069	0.035	0.033

it is clear that the attenuation will have a pressure dependence related to that of the crack density parameter.

We make the assumption, as did *Johnston et al.* [1979], that both $\bar{\nu}$ and F vary slowly with pressure and that the ratio (E/E^m) can be approximated by $(V_p/V^m_p)^2$. Using the form of ε given in (4), equation (12) is rewritten

$$Q_{cf}^{-1}(P) = TV_p^2(P)\exp(-P/\tau) \qquad (13)$$

where T is constant with pressure. Data from selected samples were also fit using two decay constants (equation (5)) to describe the pressure dependence of ε.

Note that (13) is valid only for an exponentially decaying crack density parameter. While equation (8) of *Johnston et al.* [1979] has the same form as our (12), it was not clear in their formulation what assumptions were made regarding the pressure dependence of ε, and therefore we did not use their derivation. Note that Q^{-1}_{cf} has a pressure dependence through both the velocity and the crack density parameter. We used the velocities and amplitudes measured in the rock and silica, the sample length, and the frequency f = 1 MHz to compute $Q^{-1}(P)$ using (9). Given Q^{-1}, V_p, and assuming that $Q^{-1}_c = Q^{-1}_{cf}$ and that Q^{-1}_i is constant with pressure, we substituted (13) into (11). We then fit this function to the data using a routine which iteratively adjusts the parameters Q^{-1}_i, T, and τ to minimize the least squares deviation of the function from the data.

Scattering model for attenuation. Scattering occurs if the radius of a crack is large compared to the wavelength of the propagating wave and is greatest for a wave propagating normal to the crack plane. *Kikuchi* [1981] gives an approximation for the attenuation, Q^{-1}_{cs} due to scattering by penny-shaped cracks,

$$Q_{cs}^{-1} \cong \frac{r^2 n V^m_p}{f} \qquad (14)$$

where n is the number of cracks of radius r per unit volume and V^m_p is the compressional wave velocity of the intact rock matrix at frequency f.

We have assumed that the attenuation due to scattering in the deep, highly cracked cores (from 891.0 and 1355.6 m depth) is equal to the difference between Q^{-1} values measured in the [x] and [z] directions (i.e., we assume that a small fraction of the attenuation is caused by frictional sliding). Using the P wave velocity measured in the [z] direction at the maximum confining pressure as V^m_p, we calculated the number of cracks in the sample for three values of r (2.5 mm, 5 mm, and 10 mm) using Q^{-1} measurements taken at approximately 20-MPa confinement.

Experimental Results

Examples of the crack strain, velocity, and attenuation data for the vertical [z] direction are shown in Figures 1, 2, and 3, respectively. Measurements are shown for three core samples and the corresponding surface sample from the equivalent

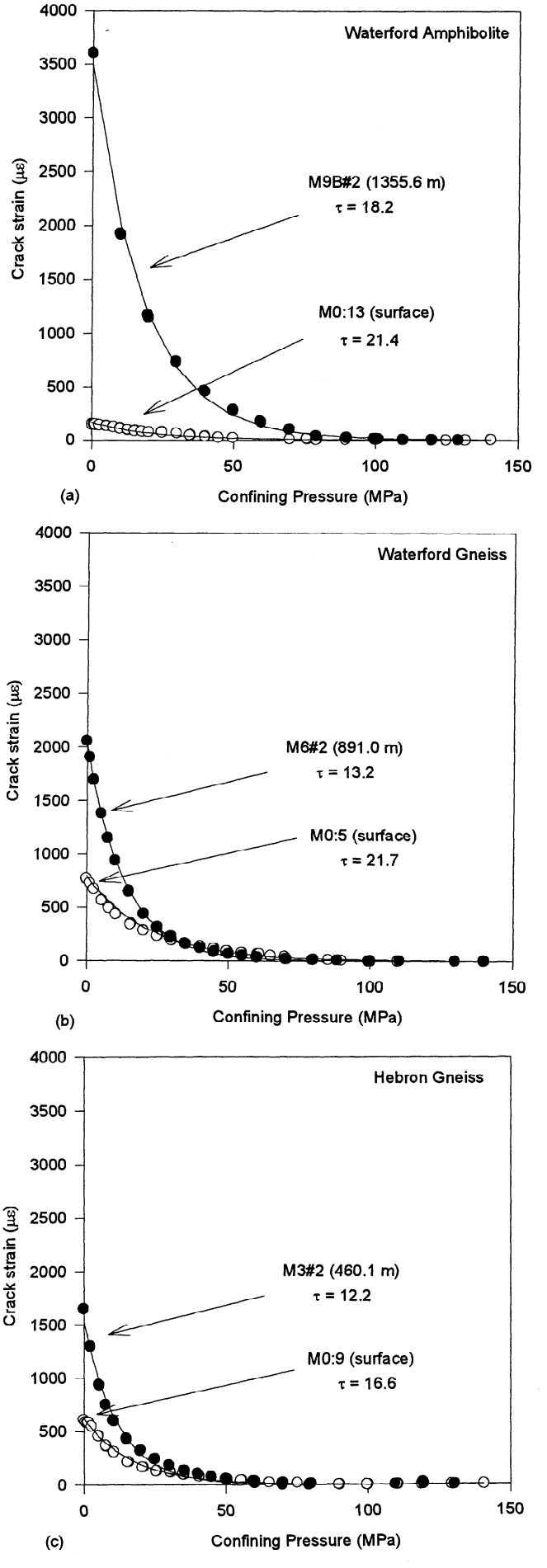

Figure 1. Examples of crack strain (η) as a function of confining pressure for selected core (solid symbol) and outcrop samples (open symbol). Curves were fit to the data using equation (3); the corresponding value of τ is shown. (a) Waterford Amphibolite, (b) Waterford Gneiss, and (c) Hebron Gneiss.

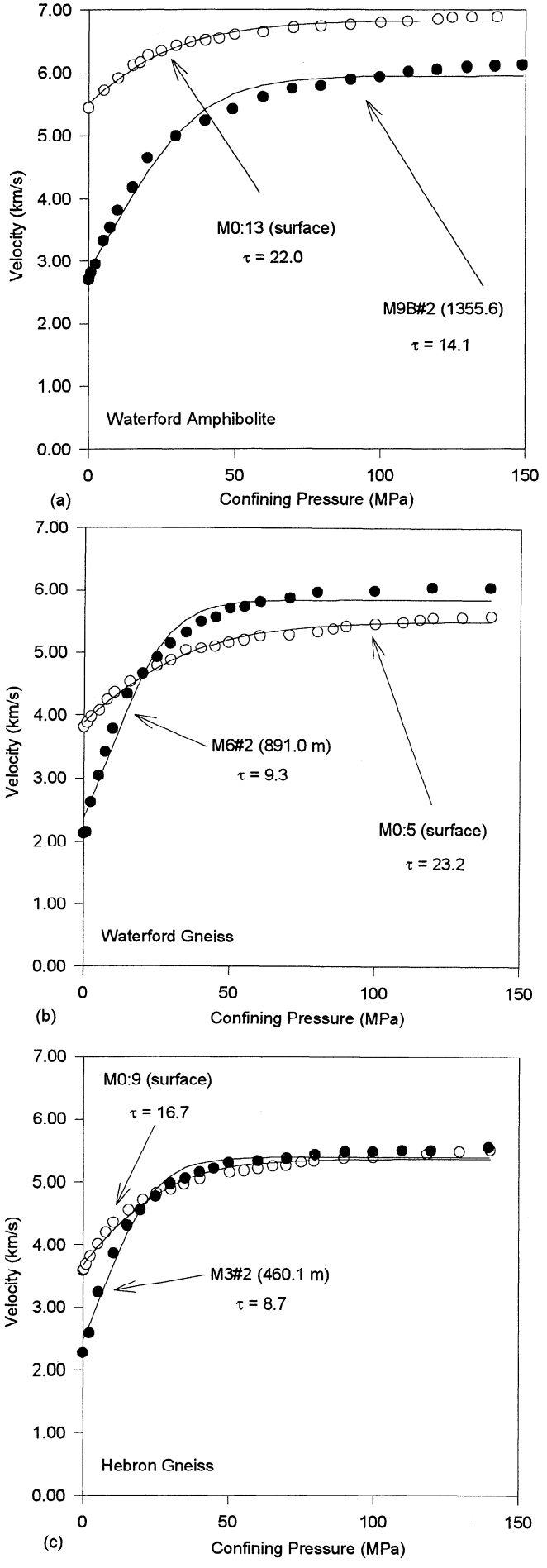

formation. Under ambient pressure conditions, the deeper cores (from 891.0 m and 1355.6 m) have larger crack strains (η) than do the shallower core (from 460.1 m) and the surface samples (Figure 1). As increasing confining pressure causes crack closure, crack strain decreases approximately exponentially in all samples. In general, the largest crack strains are measured in the vertical direction [z], parallel to the core axis, indicating a subhorizontal preferred orientation of cracks [*Meglis et al.*, 1991].

P wave velocities are lowest in all samples under ambient pressure conditions (Table 1); the core samples have lower ambient velocities than the corresponding outcrop samples (Figure 2). With increasing confining pressure, velocities increase to values between 5.50 and 7.00 km/s. The velocity anisotropy between the horizontal and vertical directions is highest at ambient pressure; the deeper samples generally have a larger velocity anisotropy at low pressures.

Q^{-1} decreases with increasing confining pressure in all samples (Figure 3). Q^{-1} measured at ambient pressure is significantly higher in the two deeper cores than in the corresponding outcrop samples. In contrast, Q^{-1} in the shallowest core and surface sample are approximately equal, even though strain and velocity measurements indicate that core sample M3#2 is more highly cracked. However, Q^{-1} is a measure of the fractional energy loss per wavelength, and because both the velocity and amplitude are lower in the core sample than in the outcrop sample, Q^{-1} is not significantly different. In the deeper cores, higher confining pressures are needed in order to reach intrinsic (Q^{-1}_i) values than in the corresponding surface samples.

Because the wave amplitude at 1 MHz is extremely low in the two deepest core samples at low pressure, approximately 20 MPa must be applied to these samples before a peak at 1 MHz can be detected. We compare Q^{-1} values measured at approximately 20 MPa with those measured at the maximum confining pressure (approximately 140-150 MPa) (Figure 4). At 20 MPa, Q^{-1} measured in the [x] direction increases slightly with sample depth (from 0.03 in the surface samples to 0.07 in the deepest core), whereas Q^{-1} measured in the [z] direction increases strongly with sample depth (from 0.03 in the surface samples to 0.22 in the deepest core). The deepest core samples show a pronounced anisotropy between the [z] and [x] directions. At the maximum pressure (140-150 MPa) confining pressure, Q^{-1} decreases in both the [z] and [x] directions to values between 0.03 and 0.05, and the difference between Q^{-1} measurements in the [x] and [z] directions diminishes significantly. Measurements of Q^{-1} in the shallow samples are consistent with published values for granites at somewhat lower frequencies (0.067 for 0.15 MHz pulse [*Blair*, 1990] and 0.049 for 0.3-0.6 MHz pulse [*Tao and King*, 1990]).

Model Results

Examples of model curves fit to the velocity, strain, and Q^{-1} measurements are overlain on the data shown in Figures

Figure 2. Examples of compressional wave velocity as a function of confining pressure for selected core (solid symbol) and outcrop samples (open symbol). Curves were fit to the data using equation (6); the corresponding value of τ is shown. (a) Waterford Amphibolite, (b) Waterford Gneiss, and (c) Hebron Gneiss.

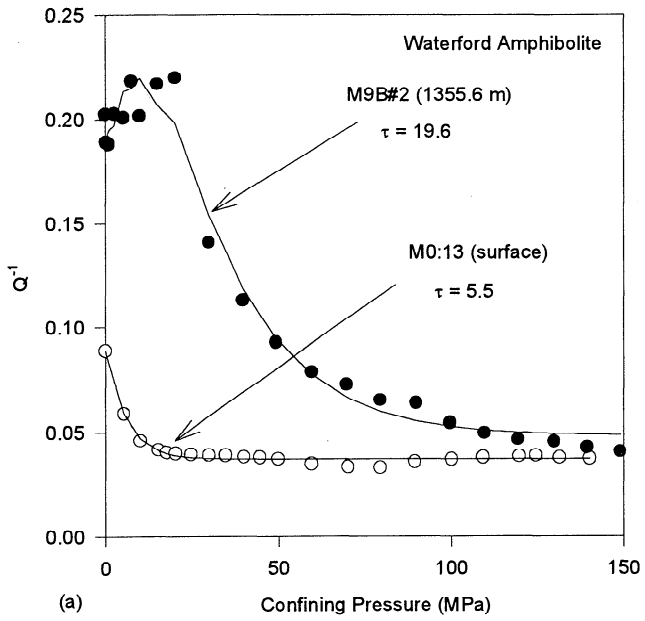

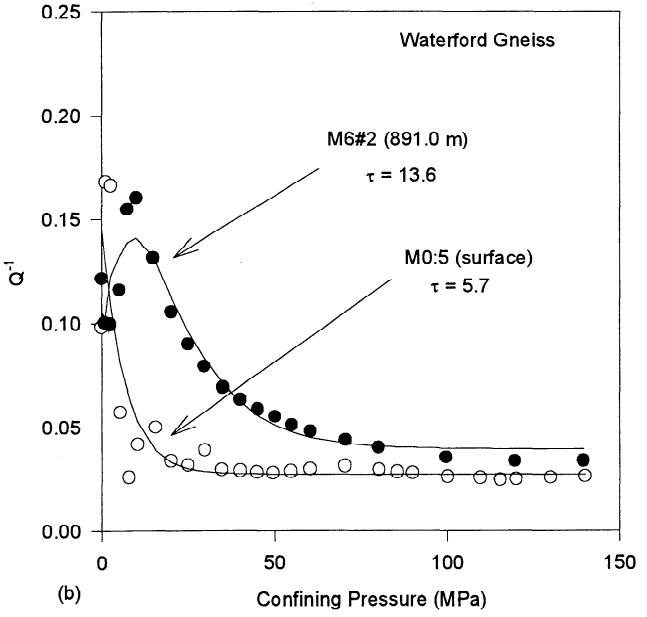

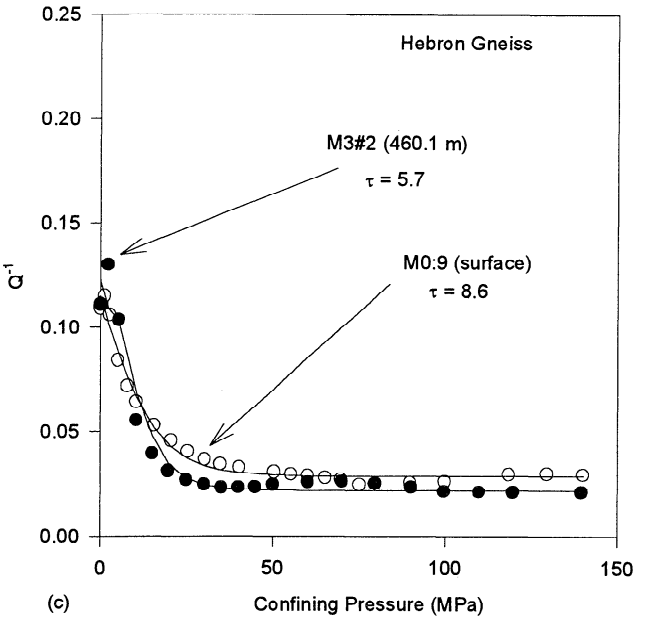

Figure 3. Examples of attenuation (Q^{-1}) as a function of confining pressure for selected core (solid symbol) and outcrop samples (open symbol). Curves were fit to the data assuming only a frictional sliding attenuation mechanism; the corresponding value of τ is shown. (a) Waterford Amphibolite, (b) Waterford Gneiss, and (c) Hebron Gneiss.

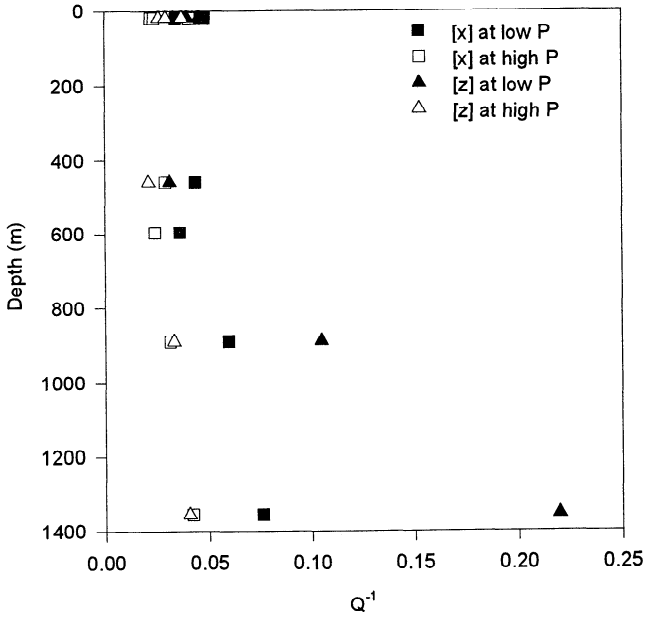

Figure 4. Q^{-1} measured in Moodus samples at 20 MPa and 140 MPa confining pressure for P waves propagating in the [x] (horizontal, N80°E) and [z] (vertical) directions.

1, 2, and 3. An exponential fit (equation (4)) is a reasonable approximation of the pressure dependence of the crack density parameter for all three measurements. However, curves fit to the velocity data using the model of *Garbin and Knopoff* [1973] (equation (6)) tend to overestimate the velocity slightly between approximately 30 and 70 MPa and underestimate it at high pressure (Figure 2). This discrepancy is more pronounced in the deeper, more highly cracked cores and led us to fit those data using a crack density parameter which is characterized by two decay constants (equation (5)). This form was necessary to reproduce the effects of both the rapid closure of cracks at low pressures and the slower closure at higher pressure.

Three model curves fit to the velocity data for sample M6#2 are plotted with the data for both the [x] and [z] directions in Figure 5. Even with the relatively large crack porosities in these samples, the models of *Hudson* [1981] and *Garbin and Knopoff* [1973] fit the data reasonably well in the [x] direction. However, in the [z] direction, equation (6) overestimates the velocity between 30 and 70 MPa and underestimates it at high pressure; using a crack density parameter with two decay constants provides a better fit to the data.

Values of τ derived from all the measurements are shown in Figures 6, 7, and 8. In general, the values of τ derived from the volumetric strain data are similar to those from the average velocity measurements fit using *Garbin and Knopoff's* [1973] velocity model (equation (6)) (Figure 6). However, for the measurements in the [x] and [z] directions

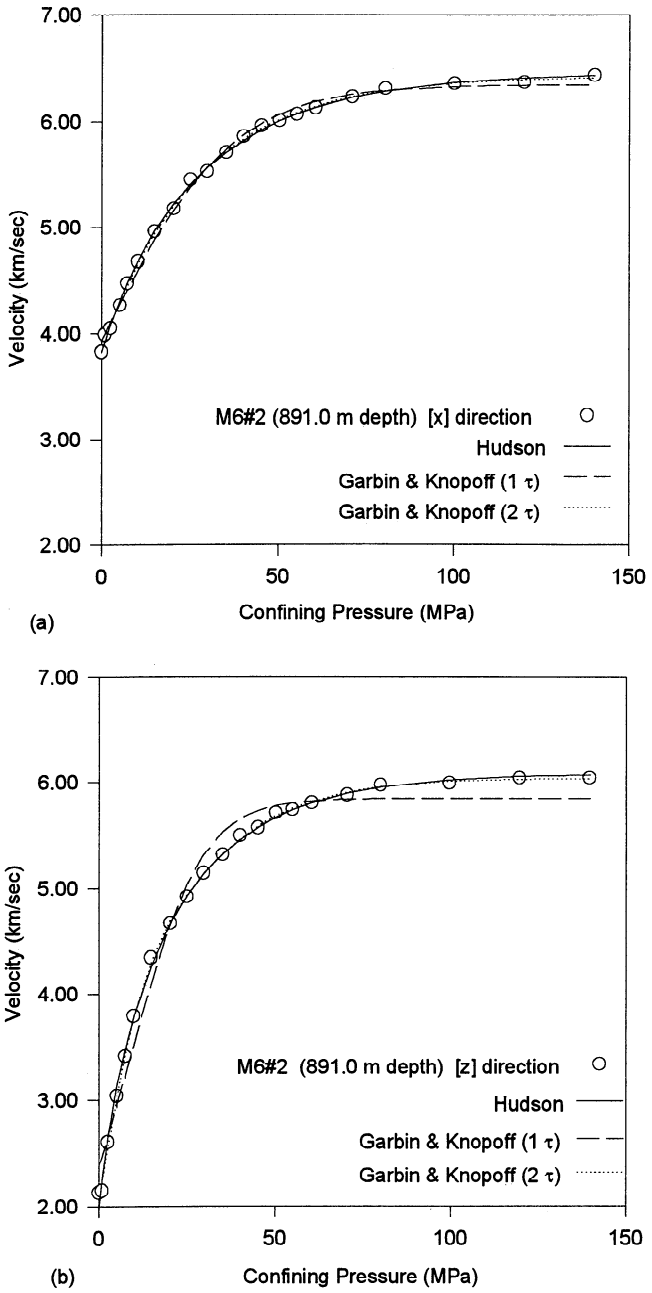

Figure 5. Comparison of curves fit to velocity data from core sample M6#2 (Waterford Gneiss from 891.0 m depth) using theory of *Garbin and Knopoff* [1973] (equation (6)) and *Hudson* [1981] (equation (7)). (a) Velocity data for the [x] direction (N80°E). (b) Velocity data for the [z] direction (vertical).

the values of τ derived from strain, velocity, and Q^{-1} for a given sample show considerable variability (Figures 7 and 8). Values of τ derived from the Q^{-1} data are lower than those from strain or the two velocity models, with the exception of data from the deep cores in the [z] direction. Values of τ for Garbin and Knopoff's velocity model are generally similar to those derived from the strain data in both the [x] and [z] directions. Values of τ derived from Hudson's velocity model are higher than those derived from Garbin and Knopoff's model. In a given sample, τ values derived from data for the [z] direction tend to be slightly lower than for data in the [x] direction. Whereas τ values derived from strain and velocity data tend to be higher in the surface samples than in the cores, the opposite is true for values derived from Q^{-1} data. There is no clear trend in τ with depth.

Results of the scattering model for attenuation are presented in Table 3. The model predicts large numbers of 2.5-mm cracks. However, the values for 10-mm-radius cracks are reasonable, since relatively long cracks (>10 mm) are visible in specimens of the deepest cores.

Discussion

With the closure of cracks under hydrostatic confining pressure, P wave velocity increases and attenuation decreases in these samples. An exponentially decreasing crack density parameter ε, used in the velocity and attenuation models, provides a reasonable fit to the data. A form which employs two decay constants provides a somewhat better fit; the difference is more substantial in the deeper, highly cracked samples. The necessity for using two τ suggests that in these samples, a population of low aspect ratio cracks (which close quickly at low pressure) is superimposed on a population which closes more slowly with pressure.

There is some variation among the τ values computed from the different data sets and models. For the velocity data, values of τ derived from *Hudson's* [1981] model (equation (7)) are larger than those from *Garbin and Knopoff's* [1973] model (equation (6)). The difference between the fits of these two models can be understood by considering the variations in velocity as a function of ε for equations (6) and (7), assuming normal incidence to a set of aligned cracks. A relatively small decrease in ε accounts for a larger velocity change in Hudson's formulation than in Garbin and Knopoff's. Therefore a larger decay constant derived from Hudson's formulation (which indicates a slower decrease in ε with pressure) is consistent with the trend of the velocity data.

The surface samples and shallow cores have undergone little stress relief during recovery and therefore have low crack porosities (Table 1). These samples generally have slightly larger values of τ for strain and velocity than the deeper core samples indicating that although the porosities are

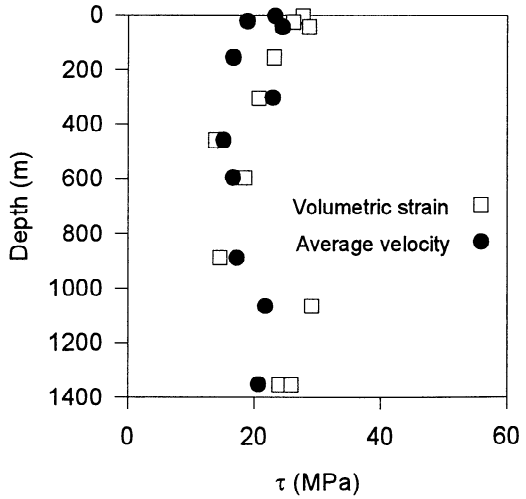

Figure 6. Plot of τ values using a single-τ fit to volumetric crack strain data and average velocity.

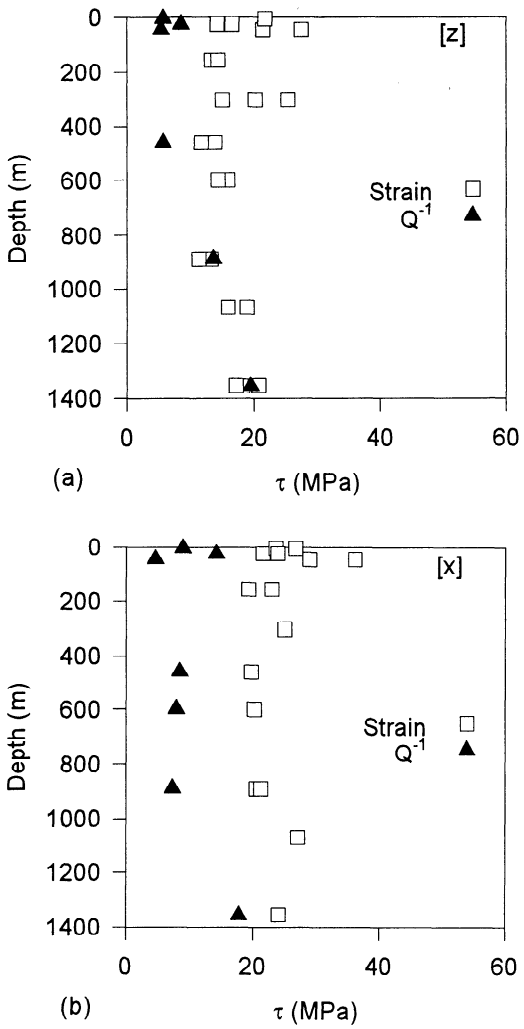

Figure 7. Plot of τ values using a single-τ fit to crack strain and Q^{-1} data, plotted at in situ depth of samples. (a) τ values computed for measurements in the [z] direction (vertical). (b) τ values computed for measurements in the [x] direction (N80°E).

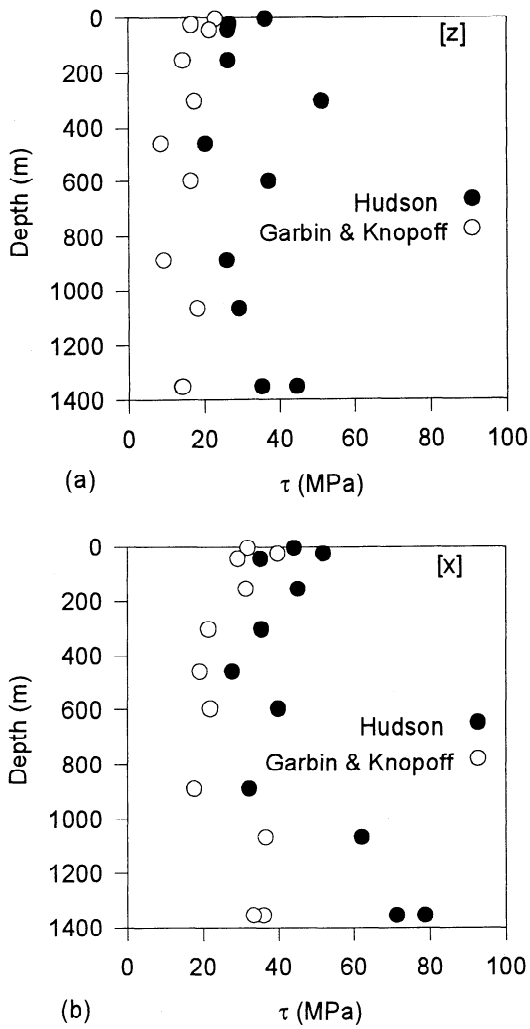

Figure 8. Plot of τ values using a single τ fit to velocity data, plotted at in situ depth of samples. (a) τ values for velocity measured in the [z] direction (vertical) using equation (6) [*Garbin and Knopoff*, 1973] and equation (7) [*Hudson*, 1981]. (b) τ values for velocity measured in the [x] direction (N80°E) using equation (6) [*Garbin and Knopoff*, 1973] and equation (7) [*Hudson*, 1981].

relatively low, the cracks persist to higher confining pressures. This behavior suggests the cracks have relatively high aspect ratios, which would be expected of partially healed cracks and pores rather than fresh, stress-induced cracks.

The deeper cores have undergone greater stress relief than the shallower samples and have been subjected to a larger stress concentration during drilling; therefore they have higher crack porosities. Furthermore, the foliation has contributed to a strong subhorizontal preferred orientation of the crack planes (normal to the [z] direction). In general, the strain and velocity data from the deeper core samples yield somewhat lower values of τ than data from the equivalent surface samples, consistent with the presence in the cores of low aspect ratio, recovery-induced cracks which close rapidly with confining pressure. In a given core sample, the vertical measurements [z] have slightly lower values of τ than the horizontal measurements [x], consistent with the preferred orientation of these cracks normal to the [z] direction.

The low τ values derived from the Q^{-1} data, compared with those from the strain and velocity data, can be understood by comparing the pressure derivatives of equations (4) and (5), since Q^{-1} behaves as $d\varepsilon/dP$. If ε is described by a single decay constant τ, its derivative will have the same decay constant. However, if the data are better fit by an ε with two decay constants, the smaller τ term will dominate the pressure derivative. Therefore approximating $d\varepsilon(\tau_1,\tau_2)/dP$ with $d\varepsilon(\tau)/dP$ yields a lower τ value for the Q^{-1} data than does

Table 3. Numbers of Cracks at Approximately 20 MPa Confining Pressure, Predicted by Scattering Model (Equation (14)) for Three Values of the Crack Radius, Computed for P Waves Propagating in the [z] Direction in Samples M6#2 and M9B#2

Sample	2.5 mm	5 mm	10 mm
M6#2	250	63	16
M9B#2	328	82	20

approximating $\varepsilon(\tau_1,\tau_2)$ with $\varepsilon(\tau)$ for the strain and velocity data.

Furthermore, the large anisotropy in crack strains and velocities between the vertical [z] and horizontal [x] directions in the deeper samples correlates with a very large anisotropy in Q^{-1} at low confining pressure (Figure 4). The anisotropy in Q^{-1} cannot be explained using *Walsh's* [1966] frictional sliding attenuation model, which predicts that for crack planes aligned approximately normal to the [z] direction, $Q^{-1}{}_z$ is not significantly larger than $Q^{-1}{}_x$. Therefore a purely frictional sliding model of attenuation is not appropriate for $Q^{-1}{}_z$ in the highly cracked samples.

The model of *Kikuchi* [1981] yields reasonable estimates of the number of large cracks which could cause the observed attenuation. We conclude that for order of magnitude estimates, Q^{-1} at low pressures in the deeper cores is primarily the result of scattering. Although the crack aperture predicted for a crack of radius 10 mm which closes at 100 MPa [*Walsh*, 1966] is relatively large (15 μm) compared to "typical" rocks [*Hadley*, 1976], the cracks in the deeper cores are large enough to be visible in hand specimens. We expect therefore that scattering may contribute to attenuation in the [z] direction even at high pressure in these samples.

Conclusions

Cracks in core and outcrop samples of crystalline rocks from the Moodus, Connecticut, area are interpreted as forming partly in response to the stress conditions imposed during sample recovery [*Meglis et al.*, 1991]. Crack porosity in the core samples is generally higher than that in the surface samples, reflecting the increasing amount of recovery-induced damage in the cores. Furthermore, a subhorizontal metamorphic foliation has contributed to a preferred alignment of crack planes normal to the core axis.

The closure of cracks under hydrostatic confining pressure, measured directly by linear strain, correlates with increasing wave velocities and amplitudes, which reach relatively constant values at high pressure. Anisotropy in velocity and attenuation diminishes with confining pressure. In order to quantify the correlation between crack closure and changes in wave velocities and amplitudes in the Moodus samples, we have employed theoretical models of wave propagation which incorporate the influence of cracks through the crack density parameter ε. The crack density parameter is approximated by an exponentially decreasing function of pressure, which has a decay constant τ. Using this form of ε in the attenuation and velocity models, we find good agreement between the measured and the predicted pressure dependence of velocity and attenuation models. However, a large anisotropy in Q^{-1} at low confining pressure in the deepest, most highly cracked cores indicates that scattering is an important attenuation mechanism. Using a model of scattering by penny-shaped cracks we find reasonable order-of-magnitude estimates for the number of cracks needed to account for attenuation at low pressure in these cores.

Acknowledgments. We thank S. J. Mackwell and Z. T. Bieniawski for reviewing an early version of this paper. This work was supported by Woodward-Clyde Consultants, the Empire State Electric Energy Research Corporation, the Electric Power Research Institute, Northeast Utilities, NSF grant EAR87-20592, the Department of the Interior's Mineral Institutes program administered by the Bureau of Mines under grant G1164142, the Pennsylvania Mining and Mineral Resources Research Institute, and by Gas Research Institute contract 5088-260-1746.

References

Batzle, M., G. Simmons, and R. W. Siegfried, Microcrack closure in rocks under stress: Direct observation, *J. Geophys. Res., 85*, 7072-7090, 1980.

Baumgartner, J., and M. D. Zoback, Interpretation of hydraulic fracturing pressure-time records using interactive analysis methods, *Int. J. Rock Mech. Min. Sci. Geomech. Abstr., 26*, 461-469, 1989.

Blair, D. P., A direct comparison between vibrational resonance and pulse transmission data for assessment of seismic attenuation in rock, *Geophysics, 55*, 51-60, 1990.

Carlson, R. L., and A. Gangi, Effect of cracks on the pressure dependence of *P* wave velocities in crystalline rocks, *J. Geophys. Res., 90*, 8675-8684, 1985.

Carlson, S. R., and H. F. Wang, Microcrack porosity and in situ stress in Illinois borehole UPH-3, *J. Geophys. Res., 91*, 10,421-10,428, 1986.

Cheng, C. H., and M. N. Toksoz, Inversion of seismic velocities for the pore aspect ratio spectrum of a rock, *J. Geophys. Res., 84*, 7533-7543, 1979.

Coyner, K. B., and R. J. Martin, Frequency dependent attenuation in rocks, final report, 44 pp., Geophys. Lab., Hanscom Air Force Base, Mass., 1990.

Crampin, S., Effective anisotropic elastic constants for wave propagation through cracked solids, *Geophys. J. R. Astron. Soc., 76*, 135-145, 1984.

Crampin, S., R. McGonigle, and D. Bamford, Estimating crack parameters from observations of P-wave velocity anisotropy, *Geophysics., 40*, 345-360, 1980.

Douglass, P. M., and B. Voight, Anisotropy of granites: A reflection of microscopic fabric, *Geotechnique, 19*, 376-398, 1969.

Engelder, T., The time-dependent strain relaxation of Algerie Granite, *Int. J. Rock Mech. Min. Sci. Geomech. Abstr., 21*, 63-73, 1984.

Engelder, T., and R. Plumb, Changes in in situ ultrasonic properties of rock on strain relaxation, *Int. J. Rock Mech. Min. Sci. Geomech. Abstr., 21*, 75-82, 1984.

Friedman, M., and T. R. Bur, Investigations of the relations among residual strain, fabric, fracture and ultrasonic attenuation and velocity in rocks, *Int. J. Rock Mech. Min. Sci. Geomech. Abstr., 11*, 221-234, 1974.

Garbin, H. D., and L. Knopoff, The compressional modulus of a material permeated by a random distribution of circular cracks, *Q. Appl. Math., 30*, 453-464, 1973.

Garbin, H. D., and L. Knopoff, The shear modulus of a material permeated by a random distribution of circular cracks, *Q. Appl. Math., 32*, 296-300,1975a.

Garbin, H. D., and L. Knopoff, Elastic moduli of a medium with liquid-filled cracks, *Q. Applied Math., 32*, 301-303,1975b.

Hadley, K., Comparison of calculated and observed crack densities and seismic velocities in Westerly Granite, *J. Geophys. Res., 81*, 3484-3494, 1976.

Hudson, J. A., Wave speeds and attenuation of elastic waves in material containing cracks, *Geophys. J. Int., 64*, 133-150, 1981.

Johnston, D. H., M. N. Toksoz, and A. Timur, Attenuation of seismic waves in dry and saturated rocks, 2, Mechanisms, *Geophysics, 44*, 691-711, 1979.

Johnston, D. H., and M. N. Toksoz, Ultrasonic *P* and *S* wave attenuation in dry and saturated rocks under pressure, *J. Geophys. Res., 85*, 925-936, 1980.

Kikuchi, M., Dispersion and attenuation of elastic waves due to multiple scattering from cracks, *Phys. Earth Planet. Inter., 27*, 100-105, 1981.

Lockner, D. A., J. B. Walsh, and J. D. Byerlee, Changes in seismic velocity and attenuation during deformation of granite, *J. Geophys. Res., 82*, 5374-5378, 1977.

Meglis, I.L., T. Engelder, and E.K. Graham, The effect of stress relief on ambient microcrack porosity in core samples from the Kent Cliffs (New York) and Moodus (Connecticut) scientific research boreholes, *Tectonophysics, 186*, 163-173, 1991.

Murphy, W. F., Seismic to ultrasonic velocity drift: intrinsic absorption and dispersion in crystalline rock, *Geophys. Res. Lett., 11*, 1239-1242, 1984.

O'Connell, R., and B. Budiansky, Seismic velocities in dry and saturated cracked solids, *J. Geophys. Res., 79*, 5412-5426, 1974.

Plumb, R., and B. Hornby, In-situ stress directions and permeable fractures in the Moodus #1 Well: Measurements from experimental ultrasonic image and Stonely wave logs. in *Moodus, CT Borehole Research Project: The magnitude and orientation of tectonic stress in southern New England, Final Report EP86-42 prepared for the Empire State Electric Energy Research Corp., Northeast Utilities, and Electric Power Research Institute*, Appendix D, Woodward-Clyde Consult., New York, 1988.

Pyrak-Nolte, L. J., L. R. Myer, and N. G. W. Cook, Anisotropy in seismic velocities and amplitudes from multiple parallel fractures, *J. Geophys. Res., 95*, 11,345-11,358, 1990.

Sayers, C. M., Inversion of ultrasonic wave velocity measurements to obtain the microcrack orientation distribution function in rocks, *Ultrasonics, 26*, 73-77, 1988.

Sayers, C. M., J. G. van Munster, and M. S. King, Stress-induced ultrasonic anisotropy in Berea Sandstone, *Int. J. Rock Mech. Min. Sci. Geomech. Abstr., 27*, 429-436, 1990.

Siegfried, R., and G. Simmons, Characterization of oriented cracks with differential strain analysis, *J. Geophys. Res., 83*, 1269-1278, 1978.

Tao, G., and M. S. King, Shear-wave velocity and Q anisotropy in rocks: A laboratory study, *Int. J. Rock Mech. Min. Sci. Geomech. Abstr., 27*, 353-361, 1990.

Toksoz, M. N., D. H. Johnston, and A. Timur, Attenuation of seismic waves in dry and saturated rocks, 1, Laboratory measurements, *Geophysics, 44*, 681-690, 1979.

Walsh, J. B., Seismic wave attenuation in rock due to friction, *J. Geophys. Res., 71*, 2591-2599, 1966.

Wang, H., and G. Simmons, Microcracks in crystalline rock from 5.3 km depth in the Michigan Basin, *J. Geophys. Res., 83*, 5849-5856, 1978.

Wepfer, W. W., and N. I. Christensen, A seismic velocity-confining pressure relation, with applications, *Int. J. Rock Mech. Min. Sci. Geomech. Abstr., 28*, 451-456, 1991.

Winkler, K., and A. Nur, Pore fluids and seismic attenuation in rocks, *Geophys. Res. Lett., 6*, 1-4, 1979.

Woodward-Clyde Consultants, *Moodus, CT Borehole Research Project: The magnitude and orientation of tectonic stress in southern New England, Final Report EP86-42 prepared for the Empire State Electric Energy Research Corp., Northeast Utilities, and Electric Power Research Institute*, New York, 1988.

T. Engelder, E. K. Graham, and R. J. Greenfield, Department of Geosciences, Pennsylvania State University, University Park, PA 16802.

I. L. Meglis, Faculty of Engineering and Applied Science, Memorial University of Newfoundland, St. John's, Newfoundland, Canada A1B 3X5. (e-mail: meglis@engr.mun.ca)

(Received June 23, 1995; revised December 4, 1995;
accepted December 28, 1995.)